2008

Shock Waves in Supersonic Two-Phase Flow of CO2 in Converging-Diverging Nozzles

Masafumi Nakagawa
Toyohashi University of Technology

Menandro Serrano Serrano
Toyohashi University of Technology

Atsushi Harada
Toyohashi University of Technology

Shock Waves in Supersonic Two-Phase Flow of CO_2 in Converging-Diverging Nozzles

Masafumi NAKAGAWA[1], Menandro Serrano BERANA[1, 2, *], Atsushi HARADA[1]

[1]Toyohashi University of Technology, Department of Mechanical and Structural System Engineering, Toyohashi City, Aichi, Japan;
Tel.: +81 (53) 244-6670, Fax: +81 (53) 244-6661, Email: berana@nak.mech.tut.ac.jp

[2]University of the Philippines-Diliman, Department of Mechanical Engineering, Quezon City, Metro Manila, Philippines;
Tel./Fax: +63 (2) 920-8875, Email: msberana@up.edu.ph (on study leave)

* Corresponding Author

ABSTRACT

CO_2 is a promising alternative to hazardous, ozone-depleting and global-warming refrigerants. It is more suitable to the ejector-refrigeration cycle than to the vapor compression cycle. However, shock waves significantly reduce the ejector-nozzle efficiency. Therefore, they must be characterized to improve the coefficient of performance and the nozzle efficiency. This paper elucidates the types of CO_2 shock waves and their relation to nozzle inlet conditions and two-phase thermodynamic states. Shock waves in supersonic liquid-vapor flows through the diverging sections of rectangular converging-diverging nozzles with the same divergence angle were investigated. They increased with supercritical inlet entropy. Equilibrium shock waves were calculated in the nozzles. The pressure behind these waves increased with decreasing diverging-section length. Two-phase-flow equilibrium shock waves, which both sides are two-phase fluid, were calculated in long nozzles. Equilibrium shock waves were very strong and thin but they were not experimentally observed. Instead, relaxation phenomena and both weak pseudo-shock waves and dispersed shock waves were experimentally observed.

1. INTRODUCTION

CO_2 has been extensively researched because it is a promising natural refrigerant. It is a potential alternative to hazardous, ozone-depleting and global-warming refrigerants (Calm and Hourahan, 2001; McQuiston *et al.*, 2005; Pearson, 2005; US EPA, 2007). The coefficient of performance (COP) obtained in using CO_2 in the ejector-refrigeration cycle is higher than that obtained in the vapor compression cycle (VCC) (Elbel and Hrnjak, 2008). Because the operation of an ejector that uses a converging-diverging nozzle includes supersonic flow, shock waves can occur at specific nozzle dimensions and flow conditions. Then, the efficiencies of the nozzle and the ejector and most importantly, the COP of the cycle are significantly reduced when shock waves occur. Therefore, their characteristics must be fully understood in order to design an efficient nozzle and ejector and improve the COP.

There are still few researches to date that characterize shock waves in supersonic two-phase flow through converging-diverging nozzles numerically and experimentally. Sugiura and Nakagawa (2001) numerically simulated shock waves in subsonic, transonic and supersonic mist flow with a constant quality of 0.01 in application to geothermal and waste-heat-recovery powerplants. They introduced a method of calculating shock waves in transonic and supersonic mist flow by using a subsonic scheme. In their model, they considered that no phase change occurred during the flow, the liquid is incompressible and the vapor is a perfect gas.

In this study, we aimed to characterize supersonic shock waves in transcritical flow of CO_2 through converging-diverging nozzles for the ejector-refrigeration cycle. The two-phase flow in this case was considered homogeneous because the flow was supersonic, the densities of the liquid and the vapor were nearly equal and the quality was about 0.5. We calculated and experimentally observed shock waves in supersonic liquid-vapor flows of CO_2 through

the diverging sections of converging-diverging nozzles. The types of shock waves of CO_2 that we obtained and their relation to inlet flow conditions and thermodynamic states in the two-phase region are presented in this paper. Hypotheses on the relation of the experimentally observed shock waves to velocity relaxation time were made.

2. EQUILIBRIUM SHOCK WAVES IN HOMOGENEOUS TWO-PHASE FLOW

2.1 Basic Governing Equations

The two-phase flow in this study was assumed to be a homogeneous mixture of liquid and vapor. For a converging-diverging nozzle shown in Figure 1, shock waves can occur in the supersonic two-phase flow in the diverging section of the nozzle. Before a shock wave occurred, it was assumed that the supersonic flow was in isentropic homogeneous expansion process. During a shock wave, it is given that the flow undergoes a non-isentropic compression. However, it was assumed that the flow remained in homogeneous state. Specifically, the velocities of the liquid and the vapor phases were assumed to be the same or in equilibrium. Hence, the shock wave created was called equilibrium shock wave. The mean specific volume v was expressed as $v = xv_g + (1 - x)v_l$. Where, v_g and v_l are the specific volumes of the vapor and the liquid phases, respectively, and x is the quality. Both phases were also assumed to have the same temperature and pressure.

As shown in Figure 1, the equilibrium shock wave was assumed to be sharp and very thin such that the change in area before and after the shock wave could be neglected. The states at the start and at the end of the shock wave were labelled as 1 and 2, respectively. The basic governing equations expressed below were derived using the formulation of Collier (1972) and applying the assumptions for homogeneous equilibrium flow mentioned above. The physical properties of the flow became a function of the temperature only because of the assumptions also.

Continuity:
$$\frac{u_1}{x_1 v_g(T_1)+(1-x_1)v_l(T_1)} = \frac{u_2}{x_2 v_g(T_2)+(1-x_2)v_l(T_2)} \tag{1}$$

Momentum:
$$\frac{u_1^2}{x_1 v_g(T_1)+(1-x_1)v_l(T_1)} + P(T_1) = \frac{u_2^2}{x_2 v_g(T_2)+(1-x_2)v_l(T_2)} + P(T_2) \tag{2}$$

Energy:
$$\frac{u_1^2}{2} + x_1 h_g(T_1) + (1-x_1)h_l(T_1) = \frac{u_2^2}{2} + x_2 h_g(T_2) + (1-x_2)h_l(T_2) \tag{3}$$

Where, u is flow velocity, T is temperature, P is pressure and h is enthalpy. The subscripts g and l refer to the vapor and the liquid phases, respectively. The above equations were numerically solved in order to analyze the equilibrium shock waves that were created. Isentropic Homogeneous Equilibrium model was used in calculating the pressure profiles before and after a shock wave occurred.

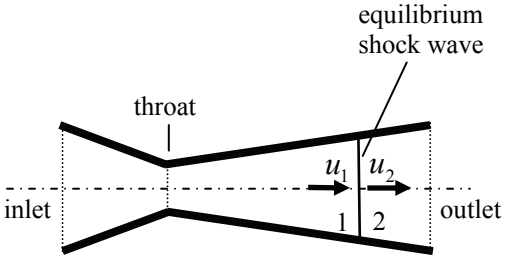

Figure 1: Equilibrium shock wave in a converging-diverging nozzle

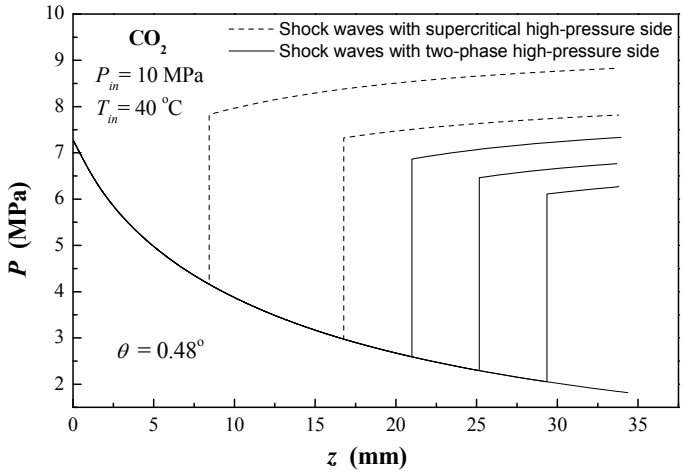

Figure 2: Equilibrium shock waves in the diverging sections of converging-diverging nozzles

2.2 Results of Numerical Simulation

The results of numerical simulation for equilibrium shock waves in the diverging sections are shown in Figure 2. Where, z is the coordinate of the flow axis of the diverging sections. Converging-diverging nozzles that had rectangular cross sectional areas with the same width were set in the simulation. The dimensions of the nozzles that were used in the simulation are shown in Figure 3. Several values of the diverging-section length $L_{divergent}$ were tried. However, the divergence angle θ was fixed at 0.48° because that was the only angle where shock waves were observed experimentally at a short nozzle length. A usual inlet condition of 10 MPa and 40°C for the ejector-refrigeration cycle was used. Physical properties of CO_2 were obtained from REFPROP (NIST, 2002). Two-phase-flow equilibrium shock waves, which are shown by solid vertical lines in Figure 2, were calculated in long nozzles using equations (1)-(3). Both sides of these equilibrium shock waves are two-phase fluid.

It was considered in the nozzle design that the equilibrium shock waves would occur at the nozzle outlets. Then, the high-pressure sides of the two-phase-flow equilibrium shock waves would be increasing with decreasing length of the diverging section. Decreasing the length would make the high-pressure side of this type of shock wave reach a supercritical state. In this case, the high-pressure side of the shock wave and the corresponding flow would become single phase. Then, no solution can be obtained from equations (1)-(3) because the right hand sides of the equations are not applicable to the supercritical region. However, these sides can be changed to expressions for single phase fluid. To solve for the properties in the supercritical region, they were chosen as functions of temperature and specific volume. From compressible single-phase flow (White, 2003), the right-hand sides of equations (1), (2) and (3) would become u_2/v_2, $u_2^2/v_2 + P(T_2, v_2)$ and $u_2^2/2 + h(T_2, v_2)$, respectively. The resulting shock waves are shown by dashed vertical lines in Figure 2. Isentropic assumption was also used after the shock waves. The supercritical high-pressure sides of these equilibrium shock waves were also increasing with decreasing diverging-section length.

There was no two-phase-flow equilibrium shock wave computed for the nozzle at an outlet pressure of about 4 MPa which is a common nozzle outlet pressure of an ejector-refrigeration cycle. Therefore, an experiment was made in order to observe the actual shock waves occurring in the nozzle. A simulated length of 8.38 mm which corresponded to the outlet pressure was used. Experiments were not made on the lengths where two-phase-flow equilibrium shock waves were computed. Those lengths corresponded to nozzle exit pressure of about 2-3 MPa which is much lower than the common nozzle outlet pressure for the cycle.

3. EXPERIMENTAL SETUP

3.1 Experimental Apparatus

The refrigeration cycle used, as shown in Figure 4, was a modified simple VCC with a compressor output power of 1.3 kW. The expansion valve was replaced by a converging-diverging nozzle to isolate the nozzle from the ejector and to easily control and investigate the inlet and the outlet states of the nozzle. The compressor, the condenser water pump and the evaporator fan were all controlled through the computer. Pressure gages and thermocouples were mounted between adjacent components.

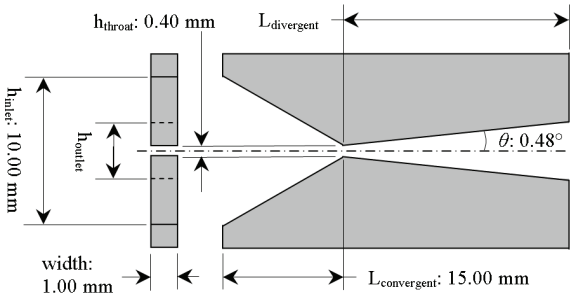

Figure 3: Dimensions of the rectangular converging-diverging nozzles used

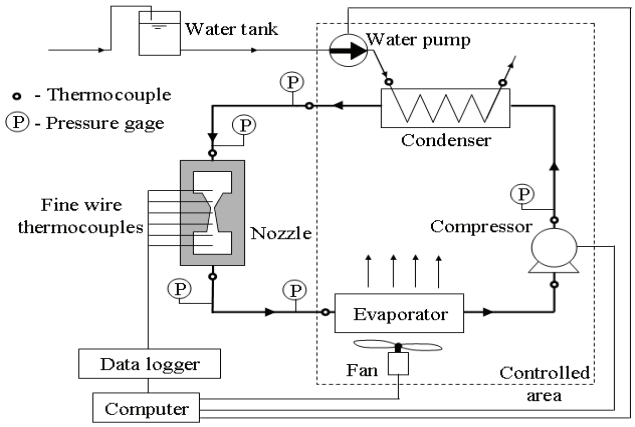

Figure 4: Experimental apparatus – the simple VCC modified by replacing the expansion valve with the converging-diverging nozzle

3.2 Nozzle Used in the Experiment

The length of the divergent section shown in Figure 3 for the experiment was decided based on numerical simulation results. It was made 8.38 mm based on Figure 2 in order to obtain a common nozzle outlet pressure of around 4 MPa for overexpanded flow. Nozzles with shorter and longer lengths were predicted to give higher and lower outlet pressure values, respectively, which are not suitable for the ejector-refrigeration cycle. The divergence angle of the nozzle was fixed to 0.48°. Overexpanded flow and shock waves were obtained at that angle for the common outlet pressure of 4 MPa and the corresponding length of 8.38 mm. Other divergence angles were tried but overexpanded flow and shock waves were not observed in the corresponding nozzles.

Thermocouple channels were inserted into drilled holes through the nozzle sidewall in order to obtain the temperature profile in the nozzle.

3.3 Experimental Procedure

Flow states of the nozzle were varied by changing the compressor frequency, the flowrate of condenser cooling water and the evaporator cooling load. When a desired flow state of the nozzle was maintained, temperatures were logged into the computer and pressures were read. CO_2 mass flowrates were calculated using heat balance in the condenser. Condenser pressures of 10-11 MPa, which are suitable for summer outdoor temperatures of up to 40°C, and evaporator pressures of 3-6 MPa were used. The resulting inlet conditions were within 9-10 MPa and 37-50°C. To determine different intensities of shock waves, the widest possible back-pressure range was obtained.

4. RESULTS AND DISCUSSIONS

The experimental results for the short nozzle are shown from Figure 5 to Figure 7. The widest possible back-pressure range obtained was 3.6-5.9 MPa. It was assumed that the flow in the converging section was isentropic. For each experimental run, the inlet entropy was determined from the corresponding actual inlet state with its pressure shown by a thick solid line. Supercritical pressures in the converging section shown by triangles were calculated using temperatures measured through the thermocouples in the section and the inlet entropy. Pressure at the throat shown by a circle was calculated by assuming that the phase change started at the throat. In that case, the flow was crossing either the saturated liquid curve or the saturated vapor curve, depending on the supercritical inlet entropy.

Inside and after the diverging section, assumed saturated pressures shown by squares were determined using corresponding temperatures measured through the thermocouples. To plot the pressure profile, inlet pressure, calculated supercritical pressures in the converging section, calculated pressure at the throat and saturated pressures inside and after the diverging section were connected using solid lines. Only one style was chosen for the data points of each profile.

The assumed start of phase change leading to saturated state in the diverging section was verified through the trend of a profile. For inlet conditions of 9 MPa, 37-45°C shown in Figure 5 and of 9.5 MPa, 40-45°C shown in Figure 6a and 6b, the start of phase change occurred at the throat. The throat pressures made smooth inflection between the partly calculated supercritical pressures in the converging section and the actual saturated pressures in the diverging section. Expansion in the diverging section was indicated by decreasing pressure from the throat. For inlet conditions of 9.5 MPa, 50°C shown in Figure 6c and of 10 MPa, 43-50°C shown in Figure 7, the start of phase change was delayed and occurring after the throat. There was no smooth inflection observed and the first measured pressures after the throat were almost the same as the throat pressures. Expansion in the diverging section and delayed start of phase change were indicated by decreasing pressure values which started further down the section.

4.1 Dependence of Shock Waves on Inlet Temperature and Inlet Pressure

The shock waves produced in the diverging section from the experiment were thick shock waves. Shock wave amplitude increased with increasing inlet temperature at a specified inlet pressure because the back pressure was increasing. Wavelength also increased because the start of shock wave went upstream in the diverging section. This trend indicated that shock wave was increasing with supercritical inlet entropy. Increasing inlet temperature at a specified inlet pressure moved an inlet condition from left to right in the supercritical region. The corresponding flow in the liquid-vapor region where shock wave occurred also moved from left to right. Conversely, shock wave was decreasing with increasing inlet pressure at a specified inlet temperature. The supercritical inlet entropy was decreasing so the effect was the opposite in this case.

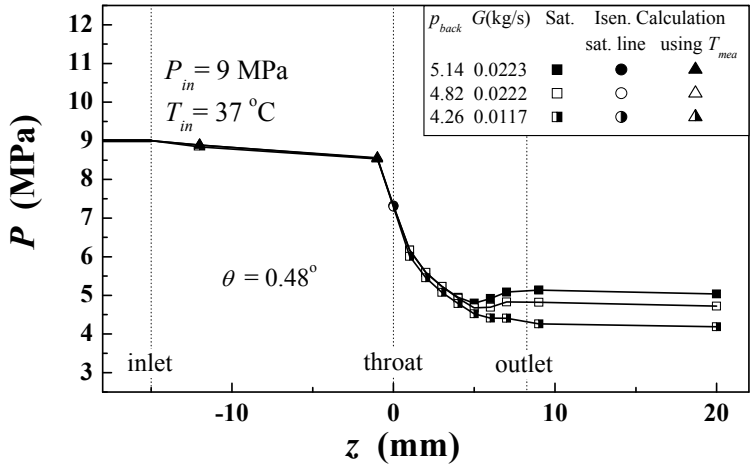

(a) Inlet at 9 MPa and 37 °C: Phase change started from saturated liquid.

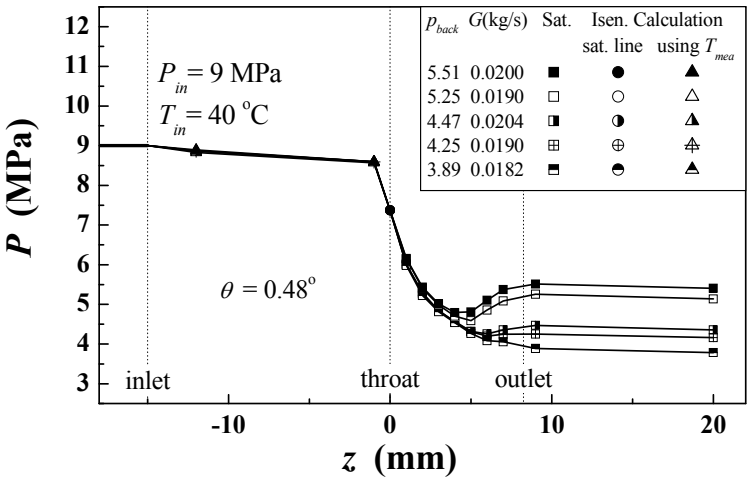

(b) Inlet at 9 MPa and 40 °C: Phase change started from saturated vapor.

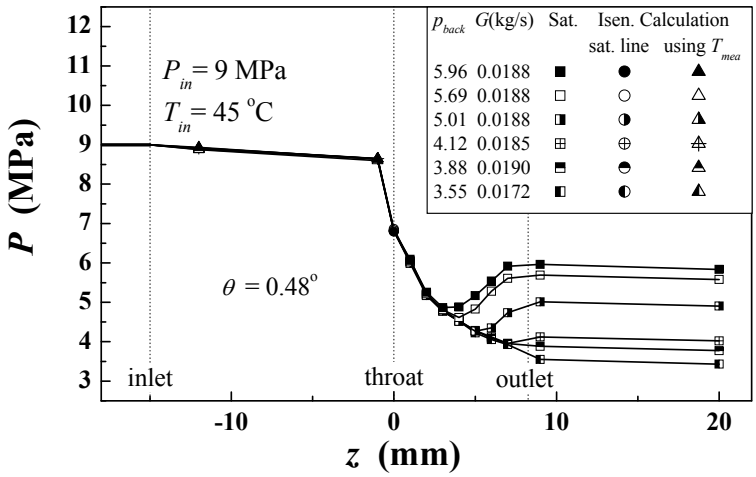

(c) Inlet at 9 MPa and 45 °C: Phase change started from saturated vapor.

Figure 5: Shock waves from the experiment at inlet conditions of 9 MPa and varying temperatures

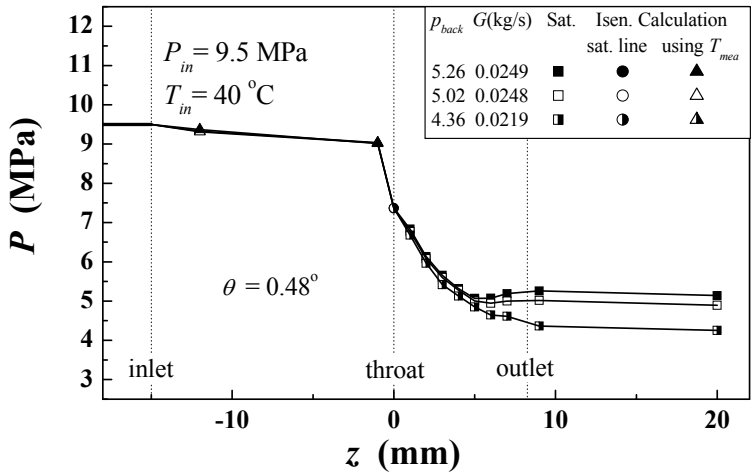

(a) Inlet at 9.5 MPa and 40 °C: Phase change started from saturated liquid.

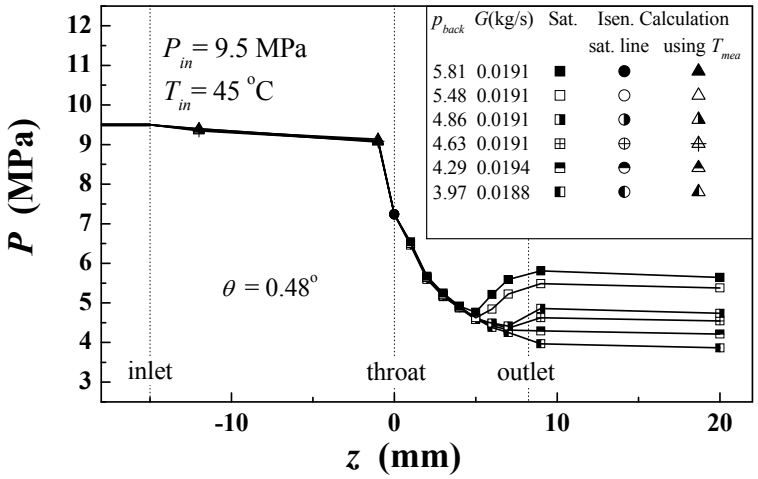

(b) Inlet at 9.5 MPa and 45 °C: Phase change started from saturated vapor.

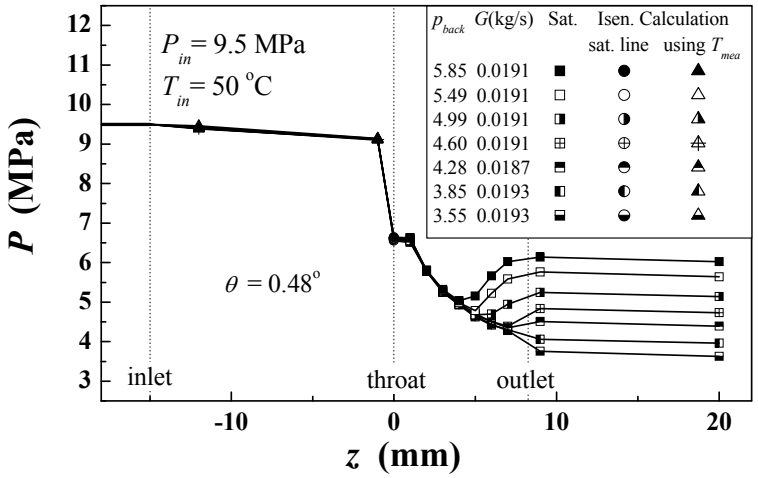

(c) Inlet at 9.5 MPa and 50 °C: Phase change started from saturated vapor.

Figure 6: Shock waves from the experiment at inlet conditions of 9.5 MPa and varying temperatures

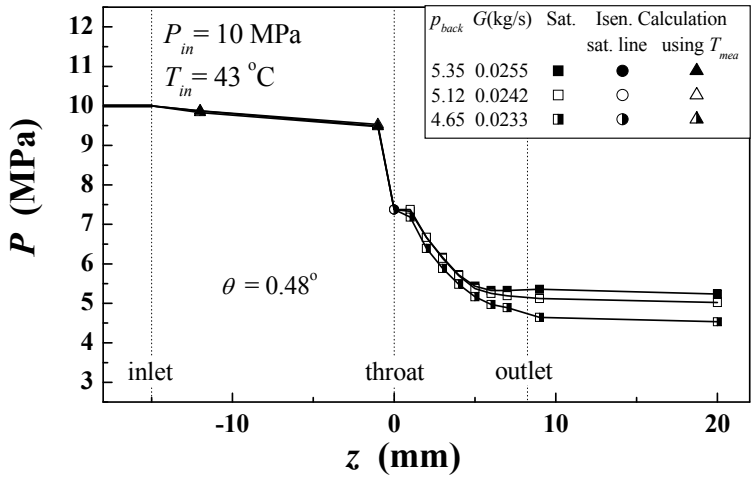

(a) Inlet at 10 MPa and 43 °C: Phase change started from saturated liquid.

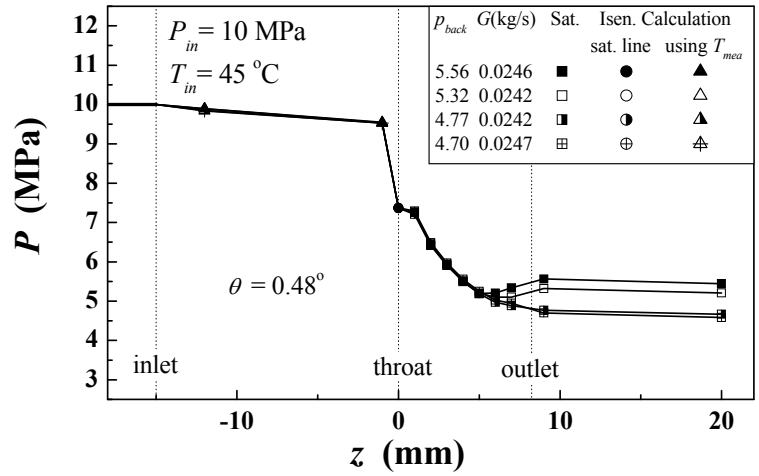

(b) Inlet at 10 MPa and 45 °C: Phase change started from saturated vapor.

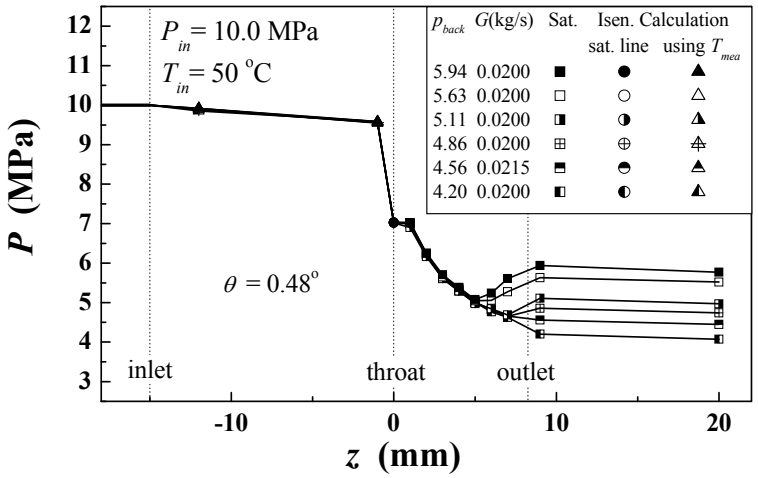

(c) Inlet at 10 MPa and 50 °C: Phase change started from saturated vapor.

Figure 7: Shock waves from the experiment at inlet conditions of 10 MPa and varying temperatures

4.2 Types of Shock Waves Appearing in the Nozzles

Strong and thin equilibrium shock waves were numerically calculated. The pressure behind these waves generally increased with decreasing diverging-section length as shown in Figure 2. Two kinds of these shock waves were determined. One was in the form of two-phase-flow equilibrium shock waves which both sides are two-phase fluid. Two-phase-flow equilibrium shock waves were calculated in long nozzles. The other was in the form of shock waves with their high-pressure sides in supercritical state. The shock waves of this kind were calculated in short nozzles. Equilibrium shock waves were not experimentally observed.

From the experiment, relaxation phenomena and two types of weak shock waves appeared in a short nozzle with a length of the diverging section of 8.38 mm and a divergence angle of 0.48°. One type was pseudo-shock wave with slight and slow increase in pressure while the other type was dispersed shock wave with moderate and gradual increase in pressure. Pseudo-shock waves shown in Figure 5a, 6a and 7a were observed in flows with supercritical inlet entropy lesser than the critical entropy. Phase change from saturated liquid to two-phase fluid was observed in this case. Oppositely, dispersed shock waves shown in Figure 5b, 5c, 6b, 6c, 7b and 7c were observed in those with supercritical inlet entropy greater than the critical entropy. Phase change from saturated vapor to two-phase fluid was observed in this case.

The relation of the experimentally observed weak shock waves to velocity relaxation was hypothesized. For pseudo-shock waves in two-phase flow, it was hypothesized that the velocity relaxation times were long. The momenta of the liquid droplets formed could not be easily decreased by the vapor. Whereas for dispersed shock waves in two-phase flow, it was hypothesized that the velocity relaxation times were short. The momenta of the gas bubbles formed could be easily decreased by the liquid.

5. CONCLUSION

Shock waves of CO_2 in supersonic two-phase flow in ejector nozzles were investigated for the ejector-refrigeration cycle. They were numerically simulated in rectangular converging-diverging nozzles with different lengths but with the same divergence angle. They were also experimentally observed in one of such nozzles with a short length. In both cases, shock waves increased with supercritical inlet entropy. Equilibrium shock waves in the nozzles were numerically calculated. The pressure behind these waves increased with decreasing diverging-section length. Two-phase-flow equilibrium shock waves, which both sides are two-phase fluid, were calculated in long nozzles. On the other hand, equilibrium shock waves with supercritical high-pressure sides were calculated in short nozzles. Equilibrium shock waves were very strong and thin but they were not experimentally observed. Instead, relaxation phenomena and weak shock waves in the forms of pseudo-shock waves and dispersed shock waves were observed in the short nozzle. For pseudo-shock waves in two-phase flow, it was hypothesized that the velocity relaxation times were long. The momenta of the liquid droplets formed could not be easily decreased by the vapor. Whereas for dispersed shock waves in two-phase flow, it was hypothesized that the velocity relaxation times were short. The momenta of the gas bubbles formed could be easily decreased by the liquid.

REFERENCES

Calm, J., Hourahan, G., 2001, Refrigerant data summary, *Engineered Systems*, vol. 18, no. 11: p 74-88.

Collier, J., 1981, *Convective Boiling and Condensation, 2nd ed.*, McGraw-Hill, New York, 435 p.

Elbel, S., Hrnjak, P., 2008, Experimental Validation of a Prototype Ejector Designed to Reduce Throttling Losses Encountered in Transcritical R744 System Operation, *Int. J. Refrig.*, vol. 31, no. 3: p. 411-422.

McQuiston, F., Parker, J., Spitler, J., 2005, *Heating, Ventilating and Air Conditioning Analysis and Design, 6th ed.*, John Wiley & Sons, New Jersey, 623 p.

NIST, 2002, *Reference Fluid Thermodynamic and Transport Properties Database (REFPROP), Version7.0*, U. S. Department of Commerce, Maryland.

Pearson A., 2005, Carbon Dioxide – New Uses for an Old Refrigerant, *Int. J. Refrig.*, vol. 28, no. 8: p. 1140-1148.

Sugiura, T., Nakagawa, M., 2001, Calculation of Supersonic Mist Flow with Shock Waves by New Subsonic Method, *The Proceedings of the International Center of Heat and Mass Transfer*, ICHMT: p. 1251-1258.

US EPA, 2007, *The Science of Ozone Layer Depletion*, http://www.epa.gov/Ozone/science/index.html.

White, F., 2003, *Fluid mechanics, 5th ed.*, McGraw-Hill, New York, 866 p.